POAC'13
Espoo, Finland

Proceedings of the 22nd International Conference on
Port and Ocean Engineering under Arctic Conditions
June 9-13, 2013
Espoo, Finland

OWEC ICE LOADS IN LANDFAST ICE ZONE

Mauri Määttänen [1] Kalle Vähätaini [2]

[1]Aalto University, Espoo, Finland and NTNU, Trondheim, Norway

[2]University of Oulu, Oulu, Finland

ABSTRACT

Land-fast ice zone offers distinct advantages for offshore wind energy converter (OWEC) foundations compared to foundations in moving ice zone. At land-fast ice zone ice is stationary most of the time during winter, especially while ice has grown thick and could exert highest loads. Wind conditions for power production are practically the same as farther away in the moving ice zone. Access to the power plants is safe and easy - especially during winter on the ice, foundations are cheaper due to smaller water depth, and power connection to mainland grid is short. However, for ice load design practice, while ice action occurs mostly in creep mode in the land-fast ice zone, both full-scale measurement data and design guidelines are missing, e.g. in ISO 19906. Observing the vast potential of easy offshore wind power in the land-fast ice zone in the Gulf of Bothnia, a joint Finnish industry project provided one full-scale wind energy converter foundation with instrumentation and a telemetry measurement system for measuring ice actions. The measurements were conducted from fall 2009 to spring 2011. This paper describes the measurement project, gathered data and data analysis. The results verify the potential of land-fast ice zone as a safe and economic area for harvesting wind power.

INTRODUCTION

In geophysics the land-fast ice zone is considered as that part of an ice covered water body where only minimal lateral ice movements occur during most of the winter period. In the arctic basins rare land-fast ice movements of several hundred meters have been reported. In the Northern Baltic during middle winter much smaller rare movements - in the order of 10 m - have occurred, typically in conjunction with storm surges (Määttänen and Kärnä, 2011). During ice formation in the fall ice cover initially moves freely. Then with increasing thickness the ice sheet gradually anchors itself to the coastline, rocks, shallows and islands, and to pressure ridge zone at the outer edge of land-fast ice zone. Thereafter thick ice can experience only short distance slow ice movements driven by thermal expansion. A rare faster ice movement may occur during such a storm surge that brings with a so high water level rise that loosens the land-fast ice. But also this is not possible after the ice has grown beyond a certain, site dependent, thickness. The opposite occurs in the spring as ice starts to deteriorate and melt. The ice load design is bounded either by ice crushing failure at expected maximum moving ice thickness, or by the maximum load during ice creep failure. Both these design load scenarios require such ice data, which is not generally available, e.g. maximum moving ice thickness and ice velocity during thermal expansion or far ice field push. An exception is the Finnish coast in the Baltic having some of the data in a comprehensive ice atlas for the Finnish coast (Palosuo and Seinä 1982, Seinä et. al. 1996). The historical data from over 90 years includes dates for ice formation and melting, snow and ice thicknesses, and even maps

of maximum moving ice thicknesses. But also here no data exists for land-fast ice lateral moving velocities at creep mode. As a new effort The Finnish Meteorological Institute (FMI) has now started to monitor land-fast ice movement at four locations in Finland.

If the design at the land-fast ice zone is based only on maximum ice thickness and ice failure in crushing mode, the result will predict excessive design loads. Timco et.al. 2003 has analysed Molikpaq data and concluded that even at quasi-stationary land-fast ice the loads are significantly lower. The thermal expansion rates could be numerically modelled provided that data exists on air temperature, wind velocities, and snow cover thickness histories. Then, as the geometry of ice field and its connections to shoreline are known, numerical models can estimate the ice velocity by assuming the initial static ice temperature profile and calculating its change. This approach includes many uncertainties. No data has been presented on land-fast ice velocity dependence on driving wind and storm surge water level rise.

A large land-fast ice zone prevails every winter along the Finnish coast southward from the Swedish border at the Northern part of the Gulf of Bothnia, Fig. 1 and 4. This about 150 km long area is prone for good wind conditions – one of the best in Finland, sea depth is relatively shallow in the order of 10 m or less, bottom typically sand or moraine, its islands and coastline are mostly inhabited. As such this land-fast ice area is rather ideal for wind power production. The potential is huge: assuming only 1/3-nominal capacity of a today's wind power plant the area could produce in average sense all the present annually needed electricity in Finland. By now several offshore wind-energy parks are already in full operation or new ones under construction elsewhere in the world. The presence of ice increases OWEC foundation cost with design uncertainty, even in the Southern part of the Baltic, that has made ice infested waters less competent. In Finland no true offshore wind energy plant is yet operational. The promise of land-fast ice zone has been utilized nowhere this far. In order to reduce uncertainty of OWEC ice load design in the land-fast ice zone a joint Finnish industry project was founded in 2008 to design, construct, instrument and measure ice actions on an OWEC foundation in the Northern Gulf of Bothnia. This paper describes the test structure, instrumentation, measurements, result analysis, and presents some data.

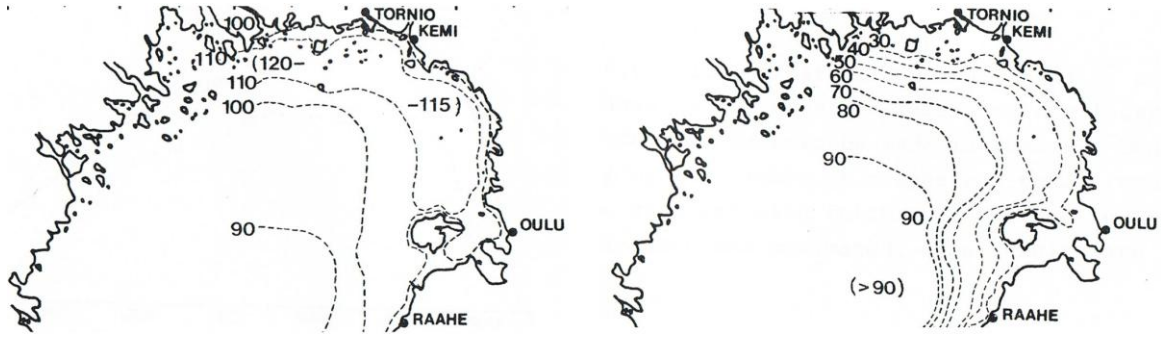

Fig.1 a) Maximum ice thickness 1920-1980 (Palosuo et.al. 1982) b) Maximum moving ice thickness

MEASUREMENT SITE IN THE LANDFAST ICE ZONE

The site for the test structure is 2 km offshore, an extension to open sea from the edge of present land based wind energy park at Ajos, close to the Kemi harbour, Fig. 1 and Fig. 2a. The location is prone to sea action from SE to SW, the direction of most severe wind actions that cause storm surges, and make the ice move in the Northern Gulf of Bothnia. The site is at the land-fast ice zone that typically consolidates in late December and prevails to May.

According to observations Fig. 1 (Palosuo et. al. 1982) the maximum moving ice thickness is 40 cm and maximum level ice thickness 1.2 m. Water level changes during storm surges can be high in open water, the maximum measured is 2.01 m on Sept 22, 1982. However, in the presence of ice cover in the Northern Baltic the storm surge is significantly lower. During the measurements from December 2009 to May 2011 the maximum winter time water level rise was 0.75 m and minimum about -0.50 m. As the coastline slope is shallow and the water level rise in the order of ice thickness one could consider this to be adequate to unlock the ad-freeze bonds and allow lateral ice movement driven by wind shear or ambient temperature changes.

The access to the test site is easy, either by boat during summer from the Ajos harbour, or during winter by various applicable vehicles on the ice. The distance is only 2 km. During the ice formation early in the winter and during final ice deterioration late in the spring an air cushion vehicle and hydro-copter were also utilized. For measurements the short distance allows to use readily available fast cellular network data-link for real time data transfer. As the sea power cable for the planned offshore wind park was not yet installed the measurement system was battery operated and charged by an aggregate.

TEST FOUNDATION AND INSTRUMENTATION

The objective was to design and manufacture an instrumented offshore wind energy converter foundation that can be furnished after the test period with a standard 3 MW wind turbine and then used in power production in the planned offshore wind energy park. To maintain true dynamic response of the tower without the final nacelle and turbine, a 180 t concrete block was installed as a replacement at +80 m level. This way the 1^{st} and 2^{nd} natural frequencies could be made identical to a complete real OWEC at 0.35 and 1.86 Hz.

The water depth to bedrock at the test site is 6.2 m. A thin sand layer above was removed, a rock pit cut, and the 5.0 m diameter steel cylinder foundation pile was fixed by concrete grouting. 29 strain gauges with their conductor wires were preinstalled to the inner surface of the foundation pile in the pile manufactures factory. The foundation and tower is basically a thin walled long cylindrical shell. Its diameter at rock pit is 5.0 m, reducing to 4,65 m at waterline and then to 3.04 m at the nacelle height. The strain gauges were installed at water line, and at -4.0 and -5.0 depths, well above rock bottom, Fig. 2c. The rationale behind chosen strain gauge locations was to measure bending moment due to global ice action, and local stress distribution due to local ice action at waterline. After the first year experiences 8 additional unidirectional strain gauges were installed at -5.0 m level evenly between the $2x45^{o}$ rosette gauges. The reason was that local ice pressures caused more complicated stress distributions in the foundation pile compared to what was assumed due to pure bending. x/y-direction accelerometers were installed both at waterline and at +80 m level. Inside the foundation pile ambient temperature and battery voltage were measured as well. A data-logger scanned all the transducers at 100 Hz and stored data to a hard disk from where it could be retrieved also in real time through a cellular phone data link. Wind data was obtained from an existing wind energy converter at coast just 2 km away.

Initially we measured ice movement manually between fixed points in x- and y-directions on ice and the test structure. As the visits to the measurement site occurred randomly the readings were recorded also at random times, and often at too long intervals. For a better accuracy a tachymeter was installed at 6 m height on the foundation pile to monitor x-y-z-distance to a laser reflector fixed about 70 m away on the solid ice, Fig. 3a and 3b. This provided continuous measurement at exact intervals. In first year the tachymeter was an independent unit and some good data was obtained late in the spring but synchronization to data logger

time was approximate. The second winter the tachymeter was coupled to the data logging system to match with the same time base of the measured strains in the foundation pile. However interface problems ruined this effort, only short data sets were recorded before the tachymeter connection was lost.

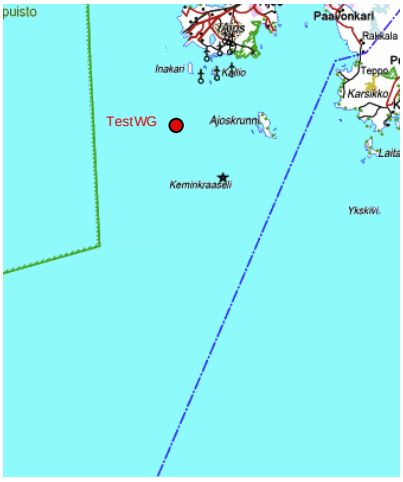

Fig. 2a. Test foundation site


Fig. 2b. Ajos test OWEC

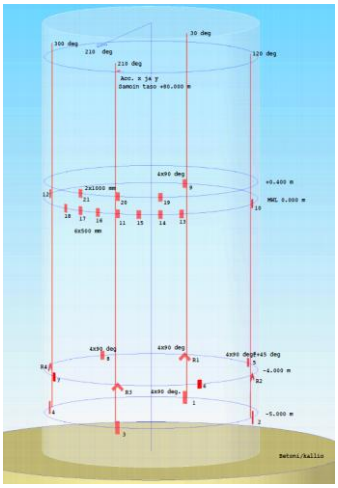
Fig. 2c. Strain gauge locations


Fig. 3a) Tachymeter installation in the door


3b) Laser reflector on the ice ≈70 m away

A pitfall in the instrumentation was the lack of continuous visual monitoring of ice actions against the foundation pile. Photos of past interaction were shot only during visits to site. A time-lapse camera would have been a cost effective but valuable asset. One problem during measurements was battery drainage. Due to more than average cold ambient temperatures the aggregate diesel motor would not always start and batteries were exhausted. A total of 10 days of data was lost. Luckily, during these periods no significant storm surges occurred.

ICE CONDITIONS

Both winters 2010 and 2011 were more severe than average. According to the Baltic ice extent related classification both measurement winters were rated as severe while the winter 2011 was close to reach to the extremely severe ice winter class. Regardless of this the land-fast ice thickness reached only to 80 cm level due to more than average snowfall. Ice formation started early, and by the end of November the land-fast ice zone had already formed. It sustained stable until final ice disappearance about mid May, Fig. 4, FMI 2010 and 2011. On 12th December 2010 ice was already 40 cm thick and grew up to 80 cm by mid March. The difference between the winters was that in 2009/2010 early heavy snow made ice surface to flood. In some locations the flooded areas froze through completely while at some other locations – those protected by thicker snowdrifts - a water layer remained between the underlying original ice and the frozen flooded layer above. In spring this caused patches of ice

to melt completely through between solid areas. Winter 2011 on the other hand had normal solid ice.

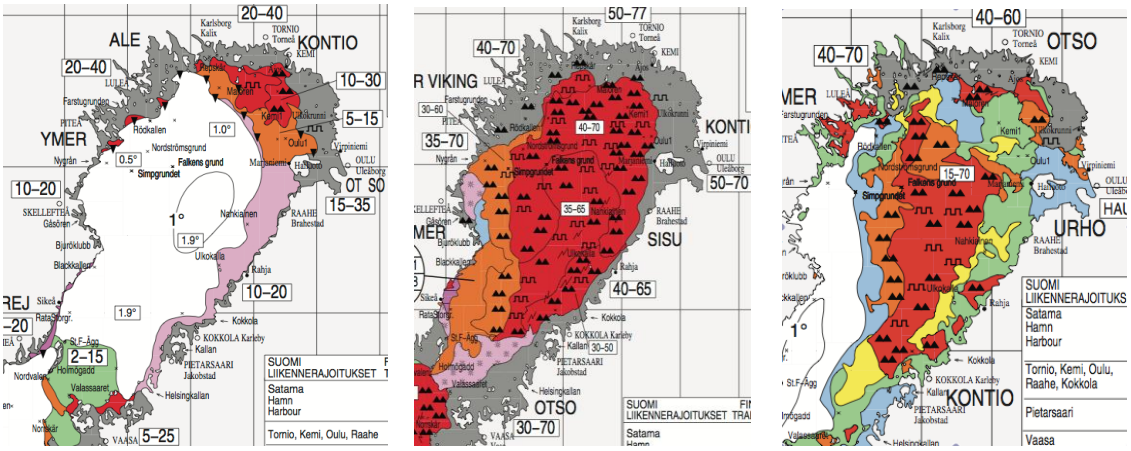

Figure 4a) 17.12.2010 4b) 19.03.2011 4c) 08.05.2011
Formation and persistence of land-fast ice zone, (FMI 2010 and 2011)

ICE MOVEMENT AND ICE FAILURE MODES

True land-fast ice movement data was captured by direct measurements during random visits to the test site and by short continuous recordings with the tachymeter. Figure 5a is a plot of manually measured ice movements during a 15 days period. Due to infrequent visits to the test site the data points are not evenly distributed with time. Fig. 5b is an 8 hours record by the tachymeter. Both data prove small total movement, in the order of ten centimetres, and the resulting ice velocity so low that ice structure interaction has been at creep range. During the whole winter on both years the total land-fast ice movement was less than 2 m.

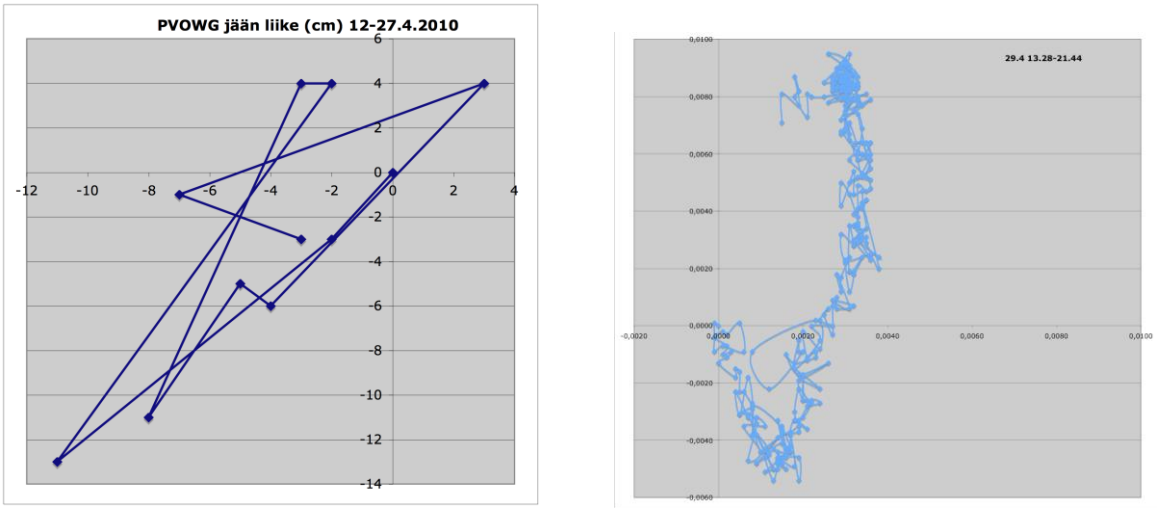

Fig. 5a) Ice movement 12-27.4.2010, manual, 5b) Ice movement 29.4.2010, tachymeter 8 hours. (Scale divisions: 5a □ 20 mm, 5b □ 2 mm, both in x- and y-directions)

In reality the land-fast ice is not stationary but experiences frequent slow lateral and vertical movements. As both the ice and the structure temperatures are most of the time under freezing point repetitive ad-freeze and failure cycles will occur. While the whole ice sheet is under environmental push from one direction the ice against the structure is creeping while on the opposite side a gap is opening, filling with water and ad-freezing. When the push ends or reverses the creep/ad-freeze process is shifting to the opposite sides. The difference of thermal

coefficient of expansion between ice and steel adds a further effect to gap filling and freezing process. E.g. a 10 ^{O}C temperature change will cause 2 mm diameter difference between the ice and the 5 m diameter foundation. With time such environmental lateral push and temperature changes with gap freezing can produce fringe patterns on the ice, Fig 6a and b.

Fig. 6a) and b) The effects of slow ice movements and temperature changes.
(6b scale: red spots 100 mm)

The water level at sea is always varying and the land-fast ice is faithfully following. When the ice is ad-frozen to the structure the rising or lowering ice level makes the ice break similarly to ice failure against a conical structure, Fig. 7a. If the ad-freeze thickness is less than ice thickness the ice sheet can split also horizontally, Fig7b. This was observed several times with the Ajos test foundation. A crushing type ice failure was never observed, Fig 7c. In crushing mode broken ice would be of random size with more or less straight failure planes.

Fig.7a) Ice bending failure 7b) Horizontal splitting 7c) No crushing

During both measurement winters no significant length land-fast ice movement occurred – not even during winter storm surges. Also in spring, the level ice melted practically in-situ by mid May, due to close presence to coastline. The effect of storm surge would be more severe late in the spring when the land-fast ice has already melted free from shoreline. However, no storm surges occurred during first part of the May while there were still large areas of solid ice remaining. Only few storm surges occurred during the measurement campaign. Daily temperature changes caused small slow ice movements. Rings of deformed ice around the foundation pile manifested such movements, Fig. 8a. The shape of broken ice pieces in a longer ice movement indicates creep type of ice deformation including both radial and horizontal splitting. The latter is most likely initiated at boundaries of water layers frozen later on top of the ice. Fig. 8b suggest slow ice movement that allows even a continuous ice protrusion in creep mode. Direct distance measurement and tachymeter data give true ice

cover displacement vectors and velocities. The data verifies very slow ice velocities up to the order of 0.1 mm/s.

Figure 8a. Fringe formation

8b. Slow ice movement with ice protrusion

ICE LOADS FROM STRAIN GAUGE DATA

The determination of ice loads from the measured strains is not straightforward even though the foundation pile is basically a long beam. Regardless that the main longitudinal bending behaviour is beamlike the real structure is a circular cylindrical shell with embedded much more complicated circular shell static behaviour. The deformations and strains are not directly proportional from the distance of bending neutral axis that would produce sinusoidal stress distributions. Shell stresses and strains depend strongly on the spatial load distribution, even far away from the load action area, e.g. FE-analysis for a 5 MPa pressure patch acting on 0,4x2,0 m^2 area at waterline, Fig 9a. Hence the ice load distribution on the pile should be known to relate measured strains into acting unknown ice loads.

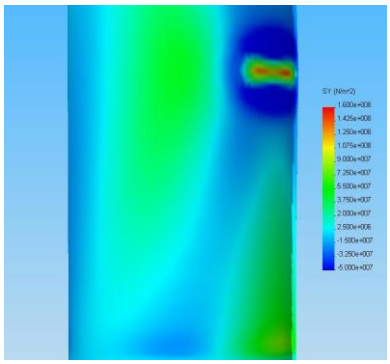

Fig. 9a. Axial stress distribution, +2…-6 m. Load at waterline. Red...Blue 160...-50 MPa

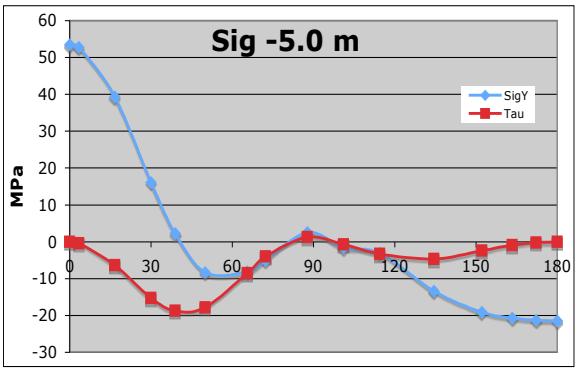

Fig. 9b. Axial and shear stress distribution at -5.0 m, a symmetric half cross section

ISO 19906 considers two ice load design cases: global ice action and local ice action. At land-fast ice zone the global action is likely to occur with perfect ice contact during slow ice movement. This is possible in ad-freeze cases and would produce a state of strain close to a sinusoidal distribution from which it would be simple to solve the global load. But the first measurements from Ajos test OWEC foundation indicated that this is not the case: the strain distributions differ significantly from a sinusoidal one. Loads due to local ice pressure are

more common and produce complicated strain distributions into the foundation pile. Local ice actions in ISO 19906 are assumed to act as constant pressure on a rectangular patch. As detailed local ice pressure measurement at waterline is practically impossible, the only chance is to compare numerically - by FE-method - predicted strain distributions to measured ones. With trial and error one can find such a local ice pressure distribution at the waterline that produces similar bending stress distribution as measured in the foundation pile cross section. By scaling the load in the FE-model by the ratio of measured and predicted strain levels the magnitude of ice load can then be solved.

MAJOR ICE ACTION EVENTS

The first ice action occurred 27-28 January 2010 while a passing low pressure centre caused heavy southern winds up to 23 m/s and raised water level 70 cm. The 80 ±1 cm thick land-fast ice at measurement site experienced two major movements northwards, first 50 cm and later 25 cm. After the storm the land-fast ice shifted back south close to its original location, Fig. 10. No signs of crushed ice in front of the test pile was present and the cavity behind the pile was already frozen during inspection at the site just after the storm on January 29, 2010, Fig.10. Fig. 11a presents the measured circumferential strain distributions with different time windows of measured axial strains at -5 m depth. One can immediately see that distributions are not sinusoidal and therefore are originating from a SW or NE-sector load. The broken ice pieces at the deformed zone were small as a result of both radial and horizontal cracking, Fig. 10. After the storm surge the land-fast ice partially retreated back close to its original position. Outside the land-fast ice zone, over 10 km south from the foundation site, the ice field had moved much faster and longer distances forming pressure ridge fields.

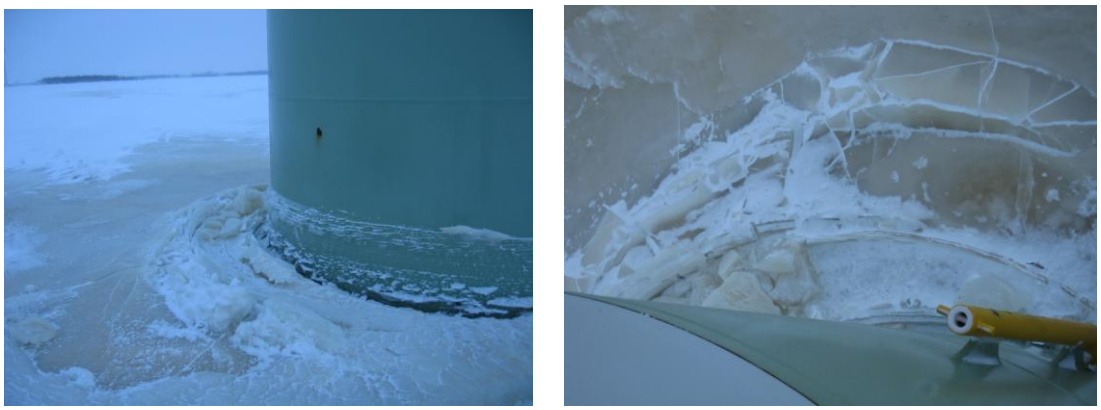

Fig.10. Ice movement patterns after the 27-28.1.2010 storm. Left SW sector and right NW sector

The recorded strains are presented in Fig. 11 for four different time periods during two days of the storm surge. Ambient temperature changes in the strain gauges and in the data logger cause thermal drift that appear as apparent strain in addition to the strains due to acting loads. This measurement error can be mostly removed by requirement that that the average strain integrated around the foundation pile cross section has to be zero. The ice load is then solved by trial: find a patch load, e.g. Fig 9a, that produces similar strain distribution to the one what has been measured. In Fig 11 the red curve, depicting a 3 h long time period strain change, results in maximum ice load during this event as it has practically no temperature change induced strains. The maximum $55*10^{-6}$ strain corresponds to the action of a less than 1 MN ice load at waterline. The violet curve during 6 hour long measurement includes so much apparent temperature drift that the true load change is less than during the red curve period.

Also the strain direction has reversed. This indicates that the violet curve present the oncoming storm surge action from SSW direction (tension at origin, 210^{O} direction) while the red results action from the retarding phase of the storm surge. The ice failure patterns in Fig. 10 at both sides of the foundation further support this kind of a back and forth movement of the land-fast ice.

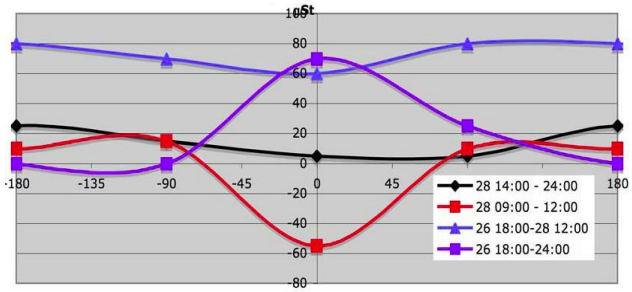

Fig.11. Foundation strain distributions at -5 m level 26-28 January 2010, (cf. FE-prediction of stresses for the half circumference in Fig. 9b).

The largest measured ice action occurred around midnight during 10 hours February 21/22. Maximum measured stresses were close to 20 MPa at -5.0 m level, Fig.12. At waterline the maximum local strains were higher causing stresses close to 50 MPa level. The maximum action point of ice pressure was gradually moving counter clockwise during this event. In reference to OWEC foundation design loads, this maximum measured static stress from land-fast ice is much smaller what a wind turbine dynamic upset load alone will cause.

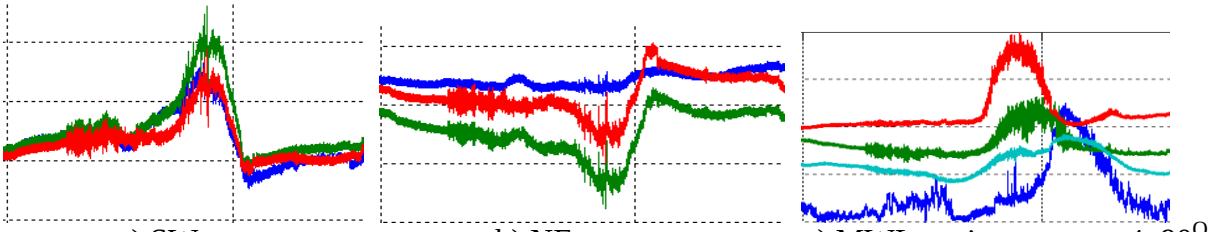

a) SW- sector b) NE - sector c) MWL strain gauges at 4x90^{O}

Fig. 12. Measured strains midnight Feb 21/22. Vertical line depicts midnight

Peculiar strain measurement events in late March and April 2011 indicate very high strain values, lower graph in Fig 13. The repeating daily waveform of strain signals at waterline and only minor effects at -4 of -5 meter depth pointed to the solar radiation effect. The southern sector of the foundation surface warmed up in the sunshine and produced significant thermal

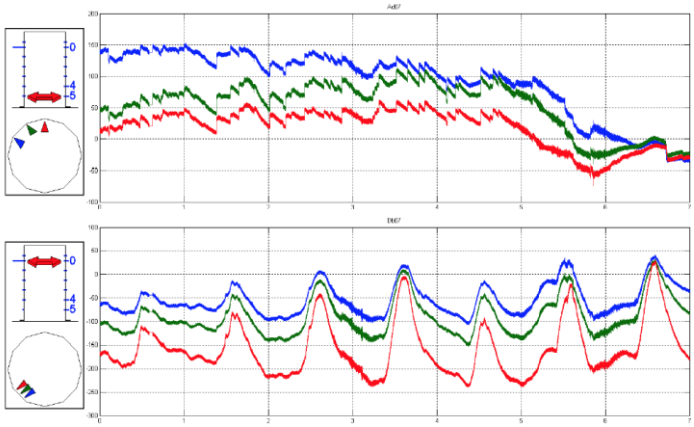

Fig.13 Strains originating from solar cycle at waterline and s at -4.0, February 14-20, 2011

strains. The resulting stresses remained small as the major effect of strains was to induce thermal expansion in the sunny side of the foundation pile and to tilt the pile above the waterline towards north. The upper graph in Fig. 13 indicates repeating stick-slip type action. There is a gradual strain change during night and many smaller short duration strain changes during daytime. These sudden changes could be explained by repetitive ice/pile adhesion failures due to push of ice on the southern sector due to larger thermal ice expansion.

Just before midnight on April 19, 2011, a significant - $230*10^{-6}$ strain p.p. - short duration (less than 20 minutes) strain oscillations occurred in otherwise quiet measurement data, Fig 14 (top). Expansion in time reveals that the strains were almost sinusoidal at 0.35 Hz which is the first natural frequency of the test structure (also with a complete OWEC on top). The wind data indicated an average of 8 m/s wind speed. With the upper foundation pile diameter 3.04 ... 4.65 m one can predict von Karman vortex street excitation to hit to resonance with the test pile lowest natural frequency of 0.35 Hz. With an operational OWEC the additional rotor aerodynamic damping effects will reduce such resonant vibration amplitudes.

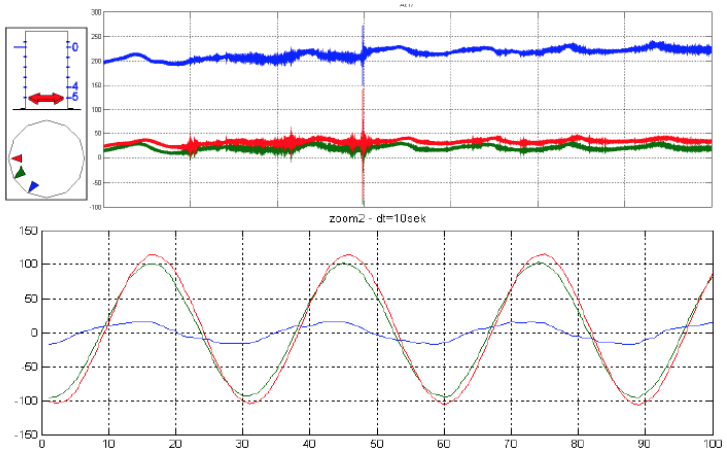

Fig. 14 Resonance peak close to midnight 19.4.2011 (top) and a 100 s sample expansion in time (below).

CONCLUSIONS

A full size instrumented OWEC foundation was designed, constructed and installed to the land-fast ice zone offshore Ajos in the Northernmost part of the Baltic. As a whole the test structure behaves both statically and dynamically as a corresponding complete OWEC. After the measurement campaign the foundation will be furnished with a nacelle and rotor for wind energy production. The test foundation was instrumented to measure continuously both static and dynamic ice actions during winters 2009-2011. The same instrumentation was used also for wave and wind load measurements.

The harvested data by telemetry measurement system includes ice actions through two winters from land-fast ice pressure during storm surges, water level changes, thermal ice expansion, solar thermal cycles, wind and wave action. Photographs during visits to test site witness various ice failure mechanisms against the foundation during short distance slow land-fast ice movements. The two winters of measurements do not cover the range of all possible ice and weather conditions for a statistical database. As such the presented data shall be considered with context to the duration and severity with the long-term ice data in the Northern Gulf of Bothnia.

The most severe ice actions occurred during storm surges. Contrary to expectations the ice action against the foundation was not around the whole ice-structure contact area but due to local patch loads. The resulting ice loads were low, significantly below the design criteria for moving ice load. Hence, in the land-fast ice zone, the overall foundation cost is close to that of an OWEC in open water without significant cost penalty due to ice actions.

The land-fast ice zone compared to moving ice zone provides many advantages for offshore wind energy production. The measurements during two years verified the low level of ice loads, absence of dynamic ice loads as well as pressure ridge loads. The maximum design load is bounded by the annual maximum moving ice thickness that is significantly thinner than maximum annual ice thickness. The maximum thick ice cannot not move fast with storm surges but its velocity is bounded to slow thermal expansion rate or slow movement driven by far field pressure while the land-fast ice is yielding in creep mode against its fixing points. The foundation cost is greatly reduced due to absence of pressure ridges, dynamic ice loads, reduced thickness of moving ice, and creep controlled loads in thick ice. In addition, the presence of an offshore wind energy park will further enhance the stability of the land-fast ice zone. The potential of land fast ice zone for offshore wind power production in ice-infested waters is proven.

ACKNOWLEDGEMENTS

The authors present their gratitude to the joint Finnish industry project that carried through the design, construction, installation, and measurements of the OWEC test foundation in the Northern Baltic, at land-fast ice zone close to Ajos. The coordinating partner was PVO Innopower Oy with participating members Insinööritoimisto Lujari Oy, Insinööritoimisto Ponvia Oy, Levator Oy, Pekkaniska Oy, Rajakiiri Oy, Suomen Hyötytuuli Oy, Suomen Meri-ituuli Oy, Terramare Oy, University of Oulu, and WinWind Oy

REFERENCES

FMI (Finnish Meteorological Institute) http://en.ilmatieteenlaitos.fi/ice-conditions

Määttänen M., and Kärnä T., 2011. ISO 19906 ice crushing load design extension for narrow structures. Proc. POAC11-63.

Palosuo E., Leppäranta M., and Seinä E., 1982. Formation, thickness and stability of fast ice along the Finnish coast. Research Report No 36, Styrelsen för vintersjöfartsforskning, Helsinki and Norrköping,

Seinä A., Grönvall H., Kalliosaari S. and Vainio J. 1996. Jäätalvet 1991-1995 Suomen merialueilla. MERI Report Series of Finnish Institute of Marine Research, No 27. Merentutkimuslaitos, Helsinki,

Timco G. and Johnston M., 2003: Ice loads on Molikpaq in the Canadian Beufort Sea. CRST Vol 37.1. pp. 51-68.